Probing of Field-Induced Structures and Their Dynamics in Ferrofluids Using Oscillatory Rheology

ARTICLE *in* LANGMUIR · SEPTEMBER 2014

Impact Factor: 4.46 · DOI: 10.1021/la502878v · Source: PubMed

2 AUTHORS:

Leona Felicia
Indira Gandhi Centre for Atomic Research
7 PUBLICATIONS **37** CITATIONS

SEE PROFILE

John Philip
Indira Gandhi Centre for Atomic Research
179 PUBLICATIONS **3,163** CITATIONS

SEE PROFILE

Langmuir

Article

pubs.acs.org/Langmuir

Probing of Field-Induced Structures and Their Dynamics in Ferrofluids Using Oscillatory Rheology

Leona J. Felicia and John Philip*

SMARTS, Metallurgy and Materials Group, Indira Gandhi Centre for Atomic Research, Kalpakkam-603 102, India

Supporting Information

ABSTRACT: We probe field-induced structures and their dynamics in ferrofluids using oscillatory rheology. The magnetic field dependence of the relaxation time and crossover modulus showed two distinct regions, indicating the different microstructures in those regions. The observed relaxation at various magnetic field strengths indicates that side chains are attached to the pinned single-sphere-width chains between the rheometer plates. Our results suggest that the ferrofluid under a magnetic field exhibits a soft solidlike behavior whose relaxation is governed by the imposed strain rate and the magnetic field. Using the scaling factors obtained from the frequency and modulus at the crossover point in the oscillatory rheological measurements, the constant strain-rate frequency sweep data is superimposed onto a single master curve. The frequency scaling factor increases with the strain rate as a power law with an exponent close to unity, whereas the amplitude scaling factor is almost strain-rate-independent at high magnetic field strengths. These findings are useful for a better understanding of field-induced ordering of nanoparticles in fluids and their optimization for practical applications.

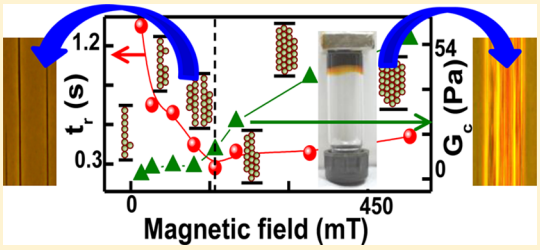

1. INTRODUCTION

Ferrofluid is a unique colloidal suspension of magnetic nanoparticles of size ranging from 5 to 15 nm that exhibits both liquid and magnetic properties.[1] Due to their interesting stimulus-responsive properties, ferrofluids have been employed in various applications, such as magneto-optical wavelength filters,[2] optical modulators,[3] nonlinear optical materials,[4] tunable optical fiber filters,[5] optical grating,[6] and defect sensors.[7] Like any other colloid, ferrofluid is a metastable system that exhibits soft glassy behavior and interesting rheological response.[8] In contrast to other soft systems,[9] dipolar fluids offer easy maneuvering with external stimuli, which makes them suitable for stimuli-responsive applications where their mechanical yield stress can be tuned by varying an external magnetic field.[10,11] Understanding the rheological properties of soft materials is very important for their effective utilization in technological applications in diverse fields.[12−15] Besides, the magnetic-field-assisted structure formation in ferrofluids is interesting from a fundamental point of view. Ferrofluid undergoes reversible phase transformation from a fluid to a viscoelastic solid under the influence of an external magnetic field. The dipolar interaction between the magnetic nanoparticles drives the aggregation of these particles into chainlike structures that are aligned along the direction of the magnetic field.[16] The linear chains undergo lateral coalescence or "zippering transitions" at higher magnetic field strength, where strong modification of rheological properties occurs.[17,18] Such tunable rheological properties have attracted considerable interest in applications like magnetofluidic seals, lubricants, density separation, inkjet printers, refrigeration, clutches, tunable dampers, and tunable heat transfer fluids.[19] Similar reversible field-induced transformations are observed in electrorheological (ER)[20] and magnetorheological (MR) fluids.[21−25] Though MR fluids exhibit superior rheological properties compared to ferrofluids in terms of yield stress, viscosity enhancement, and viscoelastic properties, they suffer drawbacks when it comes to the monodispersity of the particles and long-term stability, which are major factors controlling the rheology of suspensions. On the other hand, ferrofluids with fairly monodisperse particles and excellent long-term stability can be tailored. The magneto-rheological properties of ferrofluids have been studied both theoretically[26] and experimentally.[27,28] Though steady shear behavior of ferrofluids has been well characterized, only a few studies concentrate on their oscillatory behavior,[29,30] where the particles are considered to be noninteracting.

Many soft materials show very weak dependence of their storage modulus and loss modulus on frequency. Often the crossover from solidlike to liquidlike behavior due to low-frequency structural relaxation is difficult to detect, because such relaxation frequencies are below the accessible range of rheometers. This problem is overcome by using an approach called the strain-rate frequency superposition (SRFS), wherein the strain rate is maintained constant during the measurement.[31,32] A similar approach was used to study microscopic mechanism underlying salt-enhanced activated processes in electrostatic complexes.[33] The SRFS has been applied to a broad variety of soft materials, like suspensions,[31,34] emul-

Received: July 21, 2014
Revised: September 19, 2014
Published: September 30, 2014

sions,[34] foams,[31] polymers,[32,35] soft tissues,[36] and interfacial particle monolayers.[37] As ferrofluids are employed in many dynamic applications, insight into the dynamic rheology of ferrofluids is important. In this work we probe the relaxation dynamics in ferrofluid under magnetic field using oscillatory rheology.

2. EXPERIMENTAL SECTION

We prepared magnetite (Fe_3O_4) nanoparticles by a chemical coprecipitation technique.[38−40] The particles are sterically stabilized with a monolayer of oleic acid to prevent nanoparticle aggregation and dispersed in kerosene at a volume fraction of ϕ = 0.046. The size distribution of nanoparticles was determined by dynamic light scattering (DLS) using a Zetasizer-Nano (Malvern Instrument). The thermogravimetric analysis of the ferrofluid was carried out using a Mettler Toledo TGA/DSC system under inert atmosphere from 35 to 600 °C at a heating rate of 10 °C min^{-1}. A Carl Zeiss inverted phase-contrast microscope was used to obtain the microscopic images of the ferrofluid samples under magnetic field. Fourier transform infrared spectroscopy (FTIR) studies were done using ABB Bomem MB 3000 instrument. The spectrum was obtained in the wavenumber range from 400 to 3600 cm^{-1}. The magnetic properties of the ferrofluid were studied using a cryogen-free mini VSM (Cryogenics UK) for applied field strengths between −1.5 and 1.5 T.

From the size distribution curve (Figure 1a), the average size of the particles was found to be 13.5 nm. Figure 1b indicates that the ferrofluid sample shows three step weight losses at 143, 250, and 493 °C. The weight loss at 143 °C corresponds to the evaporation of the base fluid. The second and third step weight losses correspond to removal of the weakly and strongly bound surfactant molecules, respectively. While the carboxylic acid group of oleic acid binds to the magnetite, the aliphatic chain extends out into the nonpolar solvent, thus providing steric hindrance between the particles. There is delocalization of charges at the carboxylate ion of oleic acid in between two oxygen atoms because a resonance effect occurs. The surfactant coating thus prevents the agglomeration of particles against van der Waals and magnetic attractive interactions.

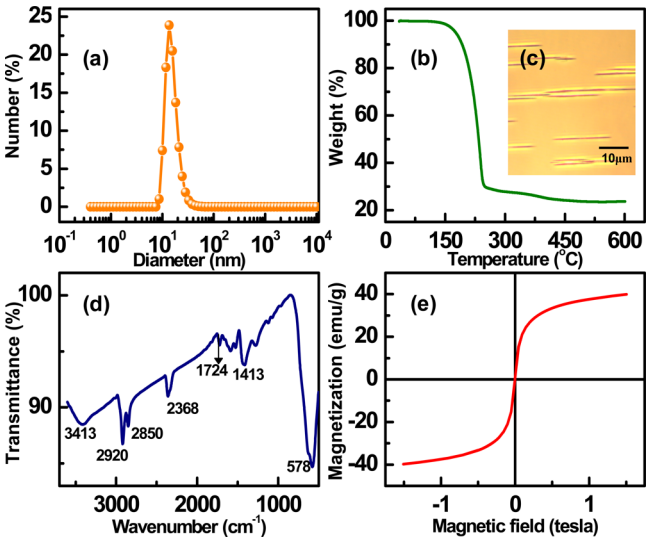

Figure 1. (a) Size distribution of the magnetite nanoparticles from DLS. (b) Thermogravimetric curve of the ferrofluid. (c) Optical phase-contrast microscopy image of the ferrofluid in the presence of magnetic field. (d) FTIR spectrum of oleic acid coated magnetite nanoparticles. (e) Magnetization curve of magnetite nanoparticles. The microscopic image was taken by diluting the original sample of ϕ = 0.046.

The microscopic image of the ferrofluid under magnetic field is shown in Figure 1c. The particles form linear chains and zippered structures aligned along the field direction. The FTIR spectrum of the magnetite particles is shown in Figure 1d, which reveals that oleic acid is chemisorbed as a carboxylate onto the Fe_3O_4 nanoparticles, and the two oxygen atoms in the carboxylate are coordinated symmetrically to the Fe_3O_4 atoms. The peak at 3413 cm^{-1} corresponds to the hydroxide ion stretching. The peaks at 2920 and 2850 cm^{-1} are due to the asymmetric and symmetric stretching, respectively, of the methylene group of the oleic acid. The peak at 1413 cm^{-1} corresponds to the asymmetric stretching of the carboxylate (COO^-) group. The peak at 578 cm^{-1} is attributed to the stretching of bonds between octahedral and tetrahedral metal ions to oxide ions,[38,41,42] while the one at 1724 cm^{-1} is due to the stretching of the C═O group of free oleic acid. Figure 1e shows the magnetization curve of the particles used in the ferrofluid. The particles are superparamagnetic with a saturation magnetization of ∼40 emu g^{-1}.

All rheological measurements are performed using a strain-controlled rheometer (Anton Paar MCR 301) with magneto-rheological attachment and a measuring system with a plate diameter of 20 mm. The stress response of the sample is measured after applying an oscillatory strain at a constant magnetic field applied perpendicularly to the plates of the rheometer. The strain-dependent measurements on the sample were carried out at different values of the magnetic field. The sample was initially subjected to a magnetic field for 2 min. The strain amplitude was then increased from 0.1 to 100% at an angular frequency of 10 rad/s, and the storage and loss moduli were recorded. The frequency-dependent measurements were performed at different magnetic fields and a fixed strain amplitude of 0.5%, which is within the linear viscoelastic (LVE) region for all the fields. The SRFS measurements were performed by simultaneously varying both the strain amplitude and frequency such that the product of the two is a constant.

3. RESULTS AND DISCUSSION

Nonlinear oscillatory studies (Figure 2a) in the presence of magnetic field (40−530 mT) show that at a constant angular frequency (ω), up to a critical strain (shown by the green arrows), the ferrofluid exhibits a strain-independent storage modulus (G'), where G' is larger than the loss modulus (G''). Above the critical strain, the storage modulus decays as a power law with strain amplitude (γ_0); i.e., $G'(\gamma_0) \propto \gamma_0^{-\upsilon'}$. The loss modulus ($G''$) exhibits a peak above the critical strain and then falls off as a power law: $G''(\gamma_0) \propto \gamma_0^{-\upsilon''}$. The ratio of the exponents, υ'/υ'', is close to 2 for all the magnetic fields. It is also observed that the critical strain marking the onset of nonlinearity decreases with magnetic field up to 160 mT and slightly increases thereafter. The response of ferrofluid to an oscillatory shear studied by Pinho et al.[29] reveals that the viscosity increases with magnetic field and monotonically decreases with oscillation frequency. A similar observation was recorded for the viscous damping force on an oscillating plate in contact with ferrofluid subjected to a constant magnetic field. The video microscopic studies in ER fluids showed that during the transition from linear to the nonlinear regime of oscillatory shear flow, the particulate columns do not break but are structurally rearranged.[43] Further simulation studies showed that the onset of nonlinearity is due to the slight rearrangements of particle clusters when the structures are sheared into unstable configurations.[44]

The linear viscoelastic measurements in Figure 2b show that the storage modulus increases with an increase in the magnetic field from 40 to 530 mT. The storage and loss moduli are weakly dependent on frequency for a magnetic field up to 160 mT. Above 160 mT, the moduli increase with increasing frequency and the storage modulus exhibited a plateau at higher

dx.doi.org/10.1021/la502878v | Langmuir 2014, 30, 12171−12179

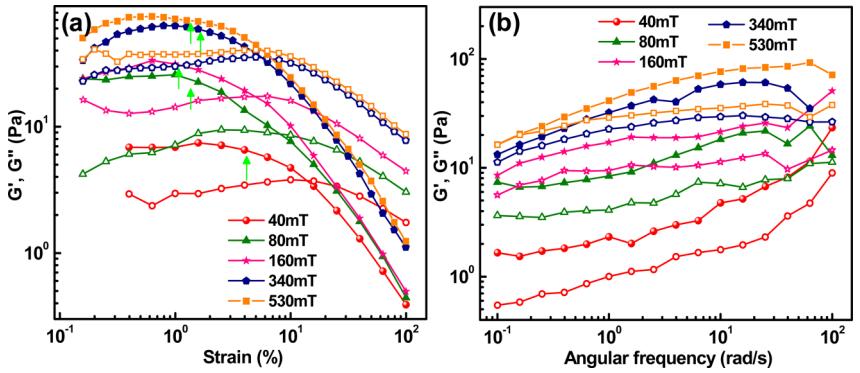

Figure 2. (a) Variation of storage and loss moduli (a) with strain amplitude and (b) with angular frequency at magnetic fields of 40, 80, 160, 340, and 530 mT. Solid symbols represent storage modulus and open symbols represent loss modulus.

frequencies. For all the magnetic fields, the storage modulus is greater than the loss modulus over the entire frequency range. However, for magnetic fields above 160 mT, a tendency to crossover is observed at the low-frequency end. The observations indicate that above 160 mT the ferrofluid exhibits short-time structural relaxation, while at lower fields the system is dominated by long-time relaxation.

Under the influence of a magnetic field, a noninteracting particle in a ferrofluid experiences hindrance to its rotation from the competing magnetic (induced dipole moments) and hydrodynamic torques.[45,46] The magnetic torque tries to align the particles' magnetic moment along the direction of the magnetic field, while the hydrodynamic one works to disrupt the alignment.[47] On the other hand, for ferrofluid containing interacting particles, the magnetic field induces the formation of chainlike structures that are aligned along the field direction when the dipolar interaction energy exceeds the thermal energy. These structures obstruct the flow, resulting in a significant enhancement in viscosity. The coupling constant λ is used to represent the effective magnetic interaction between two magnetic nanoparticles;[48] $\lambda = (\pi\mu_0 a^3 \chi^2 H^2)/(72 k_B T)$, where a is the diameter of the particle, μ_0 is the permeability of free space, H is the magnetic field strength, χ is the effective susceptibility of the nanoparticle, k_B is the Boltzmann constant, and T is the temperature. For $\lambda > 1$, magnetostatic particle interaction dominates the thermal motion, leading to the formation of chains that are aligned along the direction of the magnetic field.

As the magnetic field strength increases, the chains grow with increasing aspect ratio and span the gap between the rheometer plates.[49] The aspect ratio of the chains depends on several factors, such as the size distribution of magnetic particles, applied field strength, saturation magnetization of the particles, and volume fraction. Depending on their lengths, separations, and relative vertical positions, the chains can attract or repel one another. At high magnetic field, lateral coalescence of the chains can lead to zippering that occurs when the chains are of different lengths or shifted with respect to each other to minimize the energy. Such lateral coalescence of dipolar chains was first demonstrated by Fermigier and Gast.[17] The time scale for chain coalescence depends on the fluctuation force experienced by a chain segment and the viscous drag on the segment.[18] For moderate and highly concentrated dispersions, the coalescence time scale is much smaller than the characteristic relaxation time of the fluctuations, that is, the fluctuations persist long enough to drive the coarsening process. The modified Halsey–Toor (MHT) theory predicts lateral aggregation of two chains under large-amplitude fluctuations.[50]

The field-induced microstructural changes are reflected in the rheological properties of the ferrofluid. The increase in storage modulus with magnetic field observed in Figure 2a,b is attributed to the field-induced aggregation of particles into chains. With the number of chains increasing with field strength, the storage modulus also increases. Under a strong magnetic field, ferrofluid holds its weight on an inverted vial, which is a confirmation of the solidlike behavior. Interestingly, the loss modulus also increases with magnetic field, which is attributed to the unpinning of chains from one or both ends of the rheometer plates.[51,52] These unpinned chains have equilibrium configurations when aligned along the magnetic field. On application of rapid step shear, they may deform affinely but will relax to alignment on rheological time scales.[51,52]

In soft materials, such as hard sphere suspensions, emulsions, and foams, strain-dependent viscoelastic measurements show that beyond a critical yield strain, the storage modulus decays as a power-law while the loss modulus exhibits a peak after which it decays as a power law. The ratio (υ'/υ'') of the exponents of G' to G'' is 2.[53,54] Frequency sweep measurements show that both the storage and loss moduli are weakly dependent on frequency. A shallow minimum in the G'' near the lowest experimentally accessible frequencies followed by a pronounced maximum is considered as an indicator for a crossover from solidlike to liquidlike behavior. The frequency-independent modulus indicates that the structural relaxation occurs at a longer time scale or at very low frequency not accessible with the conventional rheometers. This problem was circumvent by Wyss et al.[31] by forcing the relaxation into an accessible frequency region using SRFS.

The structural relaxation time (τ) is related to the applied strain-rate amplitude $(\dot{\gamma}_0)$ as[31]

$$\frac{1}{\tau(\dot{\gamma}_0)} \approx \frac{1}{\tau_0} + K\dot{\gamma}_0^{\nu} \quad (1)$$

To isolate the frequency response due to structural relaxation of the soft matter system, the strain rate was maintained constant by simultaneously varying both the strain amplitude and the angular frequency. Wyss et al. observed that the response of hydrogel spheres dispersed in water shifted to higher frequencies with increasing strain-rate amplitude, while the general shape of the curves remains unaltered by $\dot{\gamma}_0$. The low-frequency response is liquidlike with $G'' > G'$, where both the

dx.doi.org/10.1021/la502878v | Langmuir 2014, 30, 12171−12179

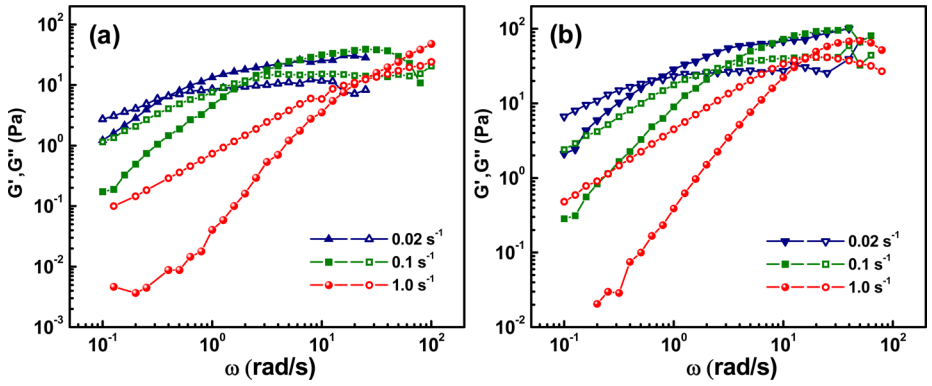

Figure 3. Frequency-dependent storage and loss moduli measured at constant strain rates of 0.02, 0.1, and 1.0 s^{-1} at (a) 160 mT and (b) 340 mT. Solid symbols represent storage moduli and open symbols represent loss moduli.

moduli scale with frequency as a power law, with a ratio of 2 between the exponents of G' and G''. In the high-frequency region, G' is greater than G'', and the storage modulus reaches a plateau, while the loss modulus shows a peak followed by a shallow minimum. Using this approach, the rescaled moduli in both magnitude and frequency were superimposed onto a single master curve. The underlying concept of this method is that factors other than the probe frequency can drive the relaxation in materials. The first ever such technique was employed in polymer melts, where the equivalence between probe frequency and temperature was used to study the dynamics of the system.[55] In this method, termed time−temperature superposition (TTS), the response of polymeric systems shifts to higher frequency by increasing the temperature. In electrostatic complexes time−salt superposition was demonstrated by Spruijt et al.,[33] where the salt concentration was the deciding factor in enhancing the process. Cramer et al.[56] demonstrated time−humidity superposition, where hydration plays a role similar to temperature in TTS. These superposition experiments reveal that probing the dynamics of the system at very low frequencies is equivalent to probing the dynamics at higher strain rate, temperature, salt concentration, or humidity, depending on the system under consideration.

The observed similarity between viscoelastic responses of ferrofluid (Figure 2) and soft materials suggests that the low-frequency response or the structural relaxation in ferrofluid can be probed by the SRFS method. The SRFS experiments were performed in the above ferrofluid system under constant values of the magnetic field at different strain rates between 0.02 and 1 s^{-1}. The results are shown in Figure 3. At a field of 160 mT (Figure 3a), for a strain rate of 0.02 s^{-1}, the high-frequency storage modulus is larger than the loss modulus and exhibits a plateau. This indicates that the suspension exhibits a solidlike nature at higher frequencies. With a decrease in frequency, both G' and G'' decrease and the response becomes liquidlike beyond a frequency of 0.38 rad s^{-1} ($G'' > G'$). This behavior is reminiscent of that of soft materials. As the strain rate increases, the crossover point shifts to a higher frequency. Thus, the previously nonobservable solidlike (elastic) to liquidlike (viscous) transition (Figure 2b) has been observed within the accessible frequency window. Similar results are observed at 340 mT, as shown in Figure 3b. The experiments performed at other magnetic fields (40 and 530 mT) also showed that the transition occurs within the accessible frequency range under constant strain rate. In the frequency region between the crossover point and the storage modulus plateau, it is seen that the G' decreases with decreasing frequency and becomes almost close to G''. In this region, the ferrofluid can be considered to exhibit a weak solidlike or gellike behavior due to a weakened microstructure.

The low-frequency moduli at different strain rates and magnetic field strengths are found to vary as a power law [$G'(\omega) \propto \omega^{-\upsilon'}$ and $G''(\omega) \propto \omega^{-\upsilon''}$]. The exponents υ' and υ'' and their ratio (υ'/υ'') at different magnetic fields and strain rates are summarized in Table 1. It is observed that at magnetic fields above 40 mT, the ratio is almost close to 2 as in the case of soft materials. In conventional frequency sweep experiments (Figure 2b), G' is weakly dependent on the frequency up to 160 mT. In the molecular dynamics simulation studies on electrorheological (ER) fluids, consisting of purely single-sphere-width chain spanning the electrode gap, G' was found to be independent of frequency and was always greater than G''.[57] It should be noted that the ER suspensions were modeled as monodisperse, neutrally buoyant, hard spheres, suspended in a Newtonian fluid held between parallel-plate electrodes. The frequency-independent G' is attributed to the zero lag between the motion of the particles in the chain and the imposed shear,

Table 1. Exponents υ' and υ'' and Their Ratio (υ'/υ'') at Different Magnetic Fields and Strain Rates

magnetic field (mT)	strain rate (s^{-1})	υ'	υ''	υ'/υ''
40	0.02	0.86	0.69	1.25
	0.05	1.06	0.71	1.49
	0.1	1.29	0.74	1.74
	0.5	1.49	0.86	1.73
	1.0	1.64	0.89	1.84
160	0.02	1.25	0.67	1.86
	0.05	1.39	0.71	1.96
	0.1	1.52	0.83	1.83
	0.5	1.49	0.92	1.62
	1.0	2.07	0.99	2.1
340	0.02	1.31	0.68	1.93
	0.05	1.44	0.78	1.85
	0.1	1.47	0.85	1.73
	0.5	1.62	0.90	1.8
	1.0	1.80	0.96	1.9
530	0.02	1.18	0.55	2.14
	0.05	1.45	0.74	1.96
	0.1	1.58	0.81	1.95
	0.5	1.66	0.91	1.82
	1.0	1.74	0.92	1.89

dx.doi.org/10.1021/la502878v | Langmuir 2014, 30, 12171−12179

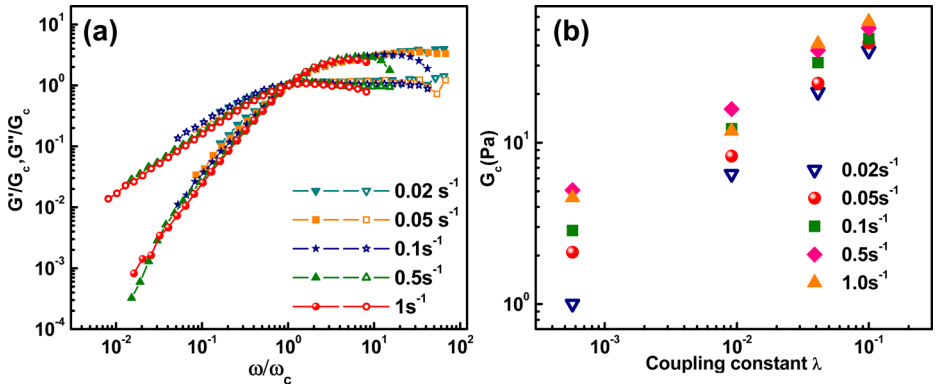

Figure 4. Constant strain-rate frequency sweep measurements shifted onto a single master curve (a) at magnetic field of 530 mT and (b) crossover modulus G_c as a function of coupling constant λ for different strain rates.

where near-zero hydrodynamic resistance leads to a non-relaxation mechanism.[57,58] On the contrary, such suspensions display a significant relaxation due to competition between hydrodynamic and electrostatic forces on spheres within the thick clusters, leading to frequency-dependent moduli. The frequency-dependent moduli observed in our case suggest that the microstructure of the ferrofluid is not composed entirely of single-sphere-width chains. The probable configuration is that small side chains are attached to the gap spanning single chains. The motion of particles in the side chain, perpendicular to the shear flow during oscillation, gives rise to a weak hydrodynamic resistance, leading to a relaxation mechanism and hence a weak frequency dependence of G'.[57]

But since the strain is less than the critical strain, the transition to nonlinearity is not witnessed and the relaxation time falls below the accessible frequency window. Above 160 mT, there is a tendency for the system to relax within the accessible frequency window, which is more pronounced at the highest applied field of 530 mT, where the storage modulus decreases from a high-frequency plateau and becomes almost close to the loss modulus value at the lowest frequency. Klingenberg[57] reported that the thick columns of particles in ER fluids exhibit frequency-dependent moduli. The loss modulus of the ER fluid increases with frequency at low frequencies, passes through a maximum, and then decreases with further increase in ω. Near the loss modulus maximum, the storage modulus increases from a low-frequency plateau value to a high-frequency plateau value. Such a low-frequency relaxation results from the large number of side chains laterally attached to the gap-spanning center chain. The competition between the hydrodynamic and magnetic forces causes the perpendicular motion of particles in the outermost chain. In the present study, the observation of a decrease in G' with decreasing frequency and the tendency to approach G'' (above a field of 160 mT) is an indication of the fact that the structures formed above 160 mT are composed of thick, zippered clusters. These clusters show a tendency to relax even under linear deformation. Thus, the above results show that the magnetic field regime can be divided into two regions, based on the types of microstructures between the parallel plates and their frequency responses. In region 1 (magnetic field range of 40−160 or 200 mT), the single-sphere-width linear chains with small side chains attached to them exist, while in the region 2 (fields ≥ 160 mT) the microstructure is dominated by thick clusters containing a greater number of side chains. Simulation studies show that the chain−chain interaction depends on the relative shift along the chain direction.[21] There are reports of formation of dense droplike aggregates in ferrofluids by López-López et al.[59] and Zubarev and Iskakova,[60] due to a condensation phase transition, where the possibility of linear chain formation is neglected because the gap between the plates (350μm) is much larger than the primary particle size (∼10 nm). These droplike aggregates span the gap between the rheometer plates, and the breaking of drops into nonspanning smaller drops occurs above a critical strain. However, in the present study, as the gap separation is much smaller (about 100 μm) compared to earlier studies, gap-spanning nanoparticle chain formation is very much possible. Such gap-spanning structures are indeed evidenced in our earlier light scattering[61] and microscopic[62] studies.

The results of the SRFS experiments (Figure 3) are discussed below. On application of SRFS at a given strain rate and magnetic field, we observe a clear transition from a low-frequency viscous response to a high-frequency elastic response (Figure 3), which was not observed in the conventional frequency sweep experiments. Here, the relaxation from the elastic behavior at high frequency to the viscous behavior at low frequency is induced by the applied strain. Parthasarathy and Klingenberg[43] reported that nonlinearity due to the rearrangement of clusters is induced by decreasing the deformation frequency by maintaining a strain greater than the critical strain. In SRFS, for a particular magnetic field, the strain amplitude exceeds the critical strain in the low-frequency region. In this region, the hydrodynamic forces appear to be negligible, while the magnetostatic force drives the particles into positions where the net force on the particle is zero at every instant. This results in the rearrangement of particles in the side chain leading to a viscous response. The rearrangement occurs due motion of the particles in the side chains during an oscillation when the competing magnetostatic and hydrodynamic forces cause the particle to move a fraction of its diameter in the direction perpendicular to shear flow.[43,57] In monodisperse ER fluids this relaxation mechanism is characterized by the time τ, which is independent of the size of the particle.[57]

As the frequency increases, hydrodynamic forces begin to dictate the particle motion. Though magnetic force influences the particle motion in the direction perpendicular to the applied shear, the time available for the structures to rearrange is not sufficient during the oscillation at such high frequencies.[57] Hence, due to nonrearrangement of particles at high frequencies, the response is linear (i.e., elastic). This explains the observed transition from low-frequency viscous

dx.doi.org/10.1021/la502878v | Langmuir 2014, 30, 12171−12179

behavior to high-frequency elastic behavior. For each magnetic field, the SRFS responses at different strain rates are rescaled in moduli and frequency as $G_{scaled} = G/G_c$ and $\omega_{scaled} = \omega/\omega_c$ using the method of Spruijt et al.[33] The scaling factors ω_c and G_c are the values of the frequency and modulus at the crossover point. It is observed that the data at all magnetic fields can be superimposed onto master curves. Figure 4 shows one such master curve obtained for a magnetic field of 530 mT. The master curves at other magnetic fields (160 and 340 mT) can be found in the Supporting Information. Indeed the curves at all magnetic fields collapse onto one single master curve (see Figure S2 in the Supporting Information), which suggests that the crossover modulus G_c also scales with the magnetic field or in turn the coupling constant (λ). The plot of G_c with λ is shown in Figure 4b. It is seen that G_c varies with λ as a power law with an exponent of 0.7, 0.58, 0.54, 0.45, and 0.5 for the strain rates of 0.02, 0.5, 0.1, 0.5, and 1 s^{-1}, respectively.

The variation of the scaling factors ω_c and G_c with strain rate for different magnetic field strengths is shown in Figure 5a,b.

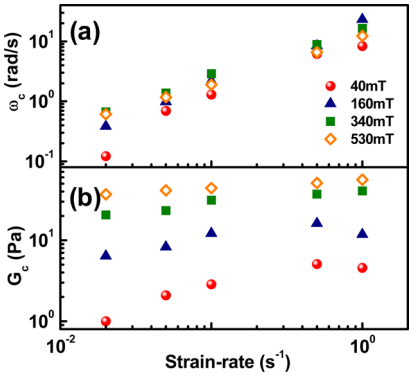

Figure 5. Scaling parameters (a) ω_c and (b) G_c as functions of strain rate for four different magnetic fields, 40, 160, 340, and 530 mT.

The frequency scaling factor (ω_c) increases with the strain rate as a power law. The exponents for the power law dependence of ω_c on strain rate are 0.9, 1.0, 0.8, and 0.8 for magnetic fields of 40, 160, 340, and 530 mT, respectively. These values are almost close to unity and are in agreement with that observed in soft materials (~1).[31] The increase in ω_c is about two orders of magnitude as the strain rate is increased from 0.02 to 1 s^{-1}. The amplitude scaling factor (G_c), on the other hand, varies weakly with the strain rate. The increase in the G_c is about half an order of magnitude for the lowest magnetic field (40 mT). As the field strength increases, G_c becomes almost strain-rate-independent. These observations imply that while the moduli values are weakly dependent on strain rate, the crossover frequency increases with the strain rate. The increase in ω_c with strain rate is attributed to the fact that the rearrangement of structures happens quickly in the presence of a larger strain rate, as the strain amplitude is higher in this case. Hence, the relaxation observed from such rearrangements is shifted to higher frequencies. Having studied the structural relaxation process in ferrofluid and the effect of strain rate on such relaxation, we proceed to probe the role of magnetic field on the relaxation phenomenon.

The magnetic field dependences of the relaxation time and G_c were analyzed by performing the SRFS experiments at a fixed strain rate by varying the magnetic field as shown in Figure 6. It was observed that, at a strain rate of 0.5 s^{-1} (Figure 6a), as the magnetic field increases up to 200 mT, the transition from the linear to nonlinear behavior shifted to higher frequencies. Above 200 mT, a decrease in the crossover frequency is noticed. Similar results were observed for SRFS experiments performed at a strain rate of 1 s^{-1} (Figure 6b).

In terms of the relaxation time t_r ($=2\pi/\omega_c$), we see that the t_r decreases with an increase in magnetic field up to ~200 mT and increases beyond this, as seen in Figure 7a. For instance, at

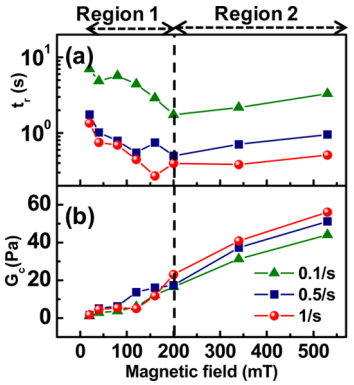

Figure 7. (a) t_r and (b) G_c as functions of magnetic field at three different strain rates, −0.1, 0.5, and 1 s^{-1}.

a strain rate of 0.1 s^{-1}, the relaxation time decreases from 4.8 to 1.7 s as the field varies from 40 to 200 mT and increases to 3.3 s at 530 mT. Similar observations were recorded at other strain rates. This shows a striking similarity with our earlier observation (Figure 2b) that the field-induced structures are

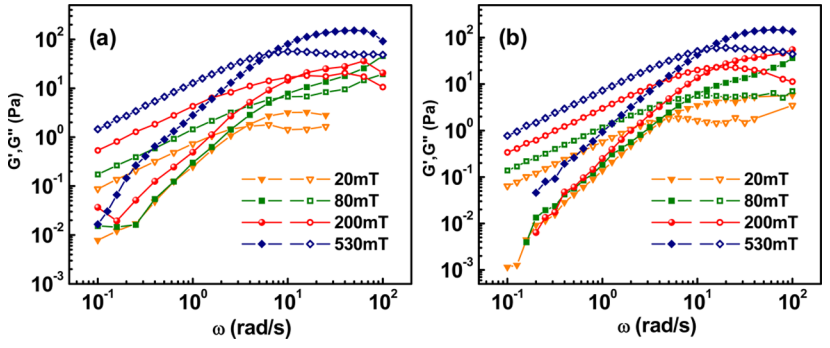

Figure 6. SRFS data under a constant strain rate of (a) 0.5 s^{-1} and (b) 1 s^{-1} at different magnetic fields. Solid symbols represent storage modulus and open symbols represent loss modulus.

dx.doi.org/10.1021/la502878v | Langmuir 2014, 30, 12171−12179

different in the two magnetic field regimes: region 1 (40−160 or 200 mT) and region 2 (≥160 mT).

The variation of t_r with magnetic field can be explained using the same argument presented in the discussion on Figure 3. In region 1, the microstructure of the ferrofluid mainly consists of gap-spanning chains with or without small side chains laterally attached (zippered chains)[63] to them, as shown in schematic Figure 8a. The controlling factors for the relaxation of the

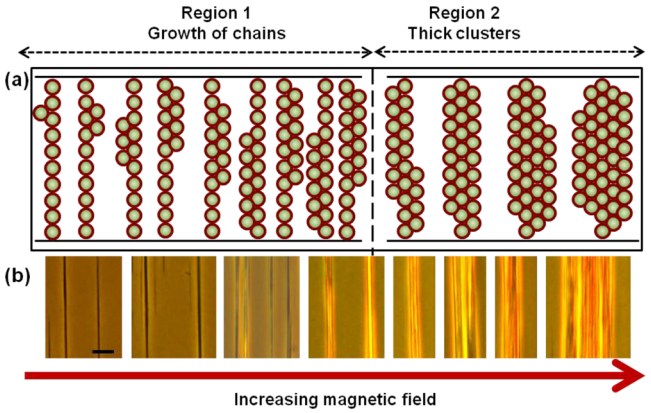

Figure 8. (a) Schematic picture of the microstructure of the ferrofluid and (b) optical phase-contrast microscopic images of the ferrofluid (ϕ = 0.046) under increasing magnetic field. The scale bar in part b corresponds to 10 μm.

structures here are the applied strain rate and magnetic field. The magnetic field defines the critical strain for transition from linear to nonlinear behavior. From Figure 2a, we observe that the critical strain decreases as the magnetic field increases up to 160 mT and increases slightly thereafter, as shown by the arrows. A decrease in critical strain with increasing electric field is also observed in ER fluids.[43] As the critical strain decreases, the domination of the hydrodynamic forces on the microstructure begins at higher frequencies, which in turn leads to a reduction in the relaxation time.

In region 2, it is observed that t_r increases with an increase in magnetic field for all the strain rates. This sudden change in the dependence of t_r on magnetic field indicates that the nature of the field-induced structures in this region is different from that in region 1. Clusters with larger sizes are known to exhibit relaxation at lower frequencies than those with smaller sizes, as particles in the outer chains undergo large excursions perpendicular to the shear flow (z direction) during oscillation.[57] The hydrodynamic resistance on these outer spheres is larger than on spheres in the side chains in region 1, resulting in restricted motion at smaller frequencies.[57] Hence, the relaxation time increases for clusters with larger thickness. This coincides with our observation of an increase in relaxation time with field in region 2, suggesting that, in this region, the thickness of the field-induced structures is larger than that of region 1. The evolution of the field-induced structures is supported by microscopic images showing few chains and their subsequent growth into thick bundles comprising a large number of chains under increasing magnetic field, as shown in Figure 8b.

Chirikov et al.[64] showed that relaxation time in ferrofluids continuously increases with magnetic field at time less than 10 s, almost similar to the results observed in our study. Kroell et al.[65] demonstrated in ferrofluid containing silica-coated magnetic nanoparticles that the relaxation time is approximately 15 s, as obtained from the maximum of the imaginary part of the complex viscosity, although the dependence of relaxation time on the magnetic field was not clear from their study. Simulation studies on ER fluids[57] also show that the time scales are almost similar to those observed in the present study. In the simulation studies by Soto-Aquino et al.[30] it was observed that despite the particles being considered to be noninteracting, an elastic response was obtained under oscillating shear. The crossover frequency denoting the transition from elastic to viscous response increased with an increase in magnetic field, indicating a decrease of the ferrofluid relaxation time with increasing magnetic field, and no increase in relaxation time at higher field was noticed.

The variation of G_c with magnetic field further supports the claim about the nature of field-induced structures in the two regions. Figure 7b shows that, for all strain rates, G_c increases weakly with magnetic field in region 1 and drastically in region 2. The microstructure in region 1 as described involves the growth process where the length of the side chains attached to the gap-spanning chain, as well as the number of such structures, increases. In region 2, the process of zippering involving the lateral coalescence of a large number of side chains occurs. This leads to the formation of clusters with greater thickness than those in region 1, giving rise to a dramatic increase in G_c with magnetic field. ER fluids also exhibit a similar increase in modulus with increasing electric field.[43] Thus, the SRFS experiments at a fixed strain rate with varying magnetic field give new insights into the nature and the evolution of field-induced structures.

Under sufficiently strong magnetic field, the Brownian and repulsive forces become negligible. At this stage, the magnetic and hydrodynamic forces dictate the rheological behavior of the ferrofluid system. The competition between these forces decides the system response. In steady shear measurements, this effect is captured by the collapse of the viscosity data when plotted against the Mason number. The details can be found in the Supporting Information (Figure S3). In oscillatory measurements this competition is revealed in both the linear and nonlinear deformations. At low strain amplitudes and low frequency, the magnetic force dominates and the response is linear. At higher strain or frequency, the hydrodynamic force begins to compete with the magnetic force, leading to an effective motion of the particles through rearrangements and hence a nonlinear behavior.

4. CONCLUSION

The field-induced structural relaxation in ferrofluid is studied using oscillatory rheology. Using the scaling factors obtained from the frequency and modulus at the crossover point in oscillatory rheological measurements, the constant strain-rate frequency sweep data is superimposed onto a single master curve. The frequency scaling factor (ω_c) increased with the strain rate as a power law with an exponent value close to unity, whereas the amplitude scaling factor (G_c) is almost strain-rate-independent at high magnetic field strengths. The structural relaxation resulting from rearrangement of particles occurred more easily as the strain rate increases. These rearrangements occur when the particles in the side chains attached to the single-sphere-width gap-spanning chain undergo motion perpendicular to the shear flow due the competition between the hydrodynamic and magnetostatic forces and is reflected as a transition from a solidlike to a liquidlike rheological response.

dx.doi.org/10.1021/la502878v | Langmuir 2014, 30, 12171−12179

The relaxation time exhibited a decrease with magnetic field up to 200 mT and an increase thereafter. The G_c, on the other hand, shows an increase with the magnetic field. The magnetic-field-dependence of the relaxation time and the crossover modulus indicates two distinct regimes. Region 1 is comprised of small and thin linear chains with a few particles attached to its side, while region 2 contains thick, zippered structures. These results suggest that the ferrofluid microstructure under magnetic field is similar to a soft solid, with relaxation governed by the imposed strain rate and the magnetic field. The new insight into relaxation behavior of field-induced aggregates in ferrofluids may have many applications, ranging from medicine to optoelectronic devices.

■ ASSOCIATED CONTENT

Supporting Information

Master curves at magnetic fields of 160 and 340 mT, single master curve at all magnetic fields (40, 160, 340 and 530 mT), viscosity curves at different magnetic fields, and Mason number collapse. These materials are available free of charge via the Internet at http://pubs.acs.org.

■ AUTHOR INFORMATION

Corresponding Author

*E-mail: philip@igcar.gov.in. Tel: 00 91 44 27480232. Fax: 00 91-44-27450356.

Notes

The authors declare no competing financial interest.

■ ACKNOWLEDGMENTS

The authors thank Dr. T. Jayakumar and Dr. P. R. Vasudeva Rao for fruitful discussions. J.P. thanks the Board of Research Nuclear Sciences (BRNS) for support through a research grant for the advanced nanofluid development program.

■ REFERENCES

(1) Rosensweig, R. E. *Ferrohydrodynamics*, 1st ed.; Dover: New York, 1997.

(2) Philip, J.; Jaykumar, T.; Kalyanasundaram, P.; Raj, B. A tunable optical filter. *Meas. Sci. Technol.* **2003**, *14*, 1289−1294.

(3) Chieh, J. J.; Yang, S. Y.; Horng, H. E.; Hong, C. Y.; Yang, H. C. Magnetic-fluid optical-fiber modulators via magnetic modulation. *Appl. Phys. Lett.* **2007**, *90*, 133505.

(4) Huang, J. P.; Yu, K. W. Magneto-controlled nonlinear optical materials. *Appl. Phys. Lett.* **2005**, *86*, 041905.

(5) Liao, W.; Chen, X.; Chen, Y.; Pu, S.; Xia, Y.; Li, Q. Tunable optical fiber filters with magnetic fluids. *Appl. Phys. Lett.* **2005**, *87*, 151122.

(6) Pu, S.; Chen, X.; Chen, L.; Liao, W.; Chen, Y.; Xia, Y. Tunable magnetic fluid grating by applying a magnetic field. *Appl. Phys. Lett.* **2005**, *87*, 021901.

(7) Mahendran, V.; Philip, J. Nanofluid based optical sensor for rapid visual inspection of defects in ferromagnetic materials. *Appl. Phys. Lett.* **2012**, *100* (7), 073104.

(8) Pastoriza-Gallego, M. J.; Pérez-Rodríguez, M.; Gracia-Fernández, C.; Piñeiro, M. M. Study of viscoelastic properties of magnetic nanofluids: An insight into their internal structure. *Soft Matter* **2013**, *9* (48), 11690−11698.

(9) Kirkland-York, S.; Gallow, K.; Ray, J.; Loo, Y.-l.; McCormick, C. Temperature induced ordering and gelation of star micelles based on ABA triblocks synthesised via aqueous RAFT polymerization. *Soft Matter* **2009**, *5*, 2179−2182.

(10) Ilg, P. Stimuli-responsive hydrogels cross-linked by magnetic nanoparticles. *Soft Matter* **2013**, *9* (13), 3465−3468.

(11) Rodrıguez-Arco, L.; Lopez-Lopez, M. T.; Kuzhir, P.; Duran, J. D. G. Steady state rheological behaviour of multi-component magnetic suspensions. *Soft Matter* **2013**, *9* (24), 5726−5737.

(12) Eberle, A. P. R.; Wagner, N. J.; Castaneda-Priego, R. Dynamical arrest transition in nanoparticle dispersions with short-range interactions. *Phys. Rev. Lett.* **2011**, *106* (10), 105704.

(13) Raghavan, S. R.; Walls, H. J.; Khan, S. A. Rheology of silica dispersions in organic liquids: New evidence for solvation forces dictated by hydrogen bonding. *Langmuir* **2000**, *16* (21), 7920−7930.

(14) Chen, D. T. N.; Wen, Q.; Janmey, P. A.; Crocker, J. C.; Yodh, A. G. Rheology of soft materials. *Annu. Rev. Condens. Matter Phys.* **2010**, *1*, 301−322.

(15) Madivala, B.; Fransaer, J.; Vermant, J. Self-Assembly and rheology of ellipsoidal particles at interfaces. *Langmuir* **2009**, *25* (5), 2718−2728.

(16) Odenbach, S. *Colloidal Magnetic Fluids: Basics, Development and Application of Ferrofluids*. Springer: New York, 2009.

(17) Fermigier, M.; Gast, A. P. Structure evolution in a paramagnetic latex suspension. *J. Colloid Interface Sci.* **1992**, *154* (2), 522−539.

(18) Furst, E. M.; Gast, A. P. Dynamics and lateral interactions of dipolar chains. *Phys. Rev. E* **2000**, *62* (5), 6916−6925.

(19) Shima, P. D.; Philip, J. Tuning of thermal conductivity and rheology of nanofluids using an external stimulus. *J. Phys. Chem. C* **2011**, *115* (41), 20097−20104.

(20) Klingenberg, D. J.; Z, IV Studies on the Steady-Shear Behavior of Electrorheological Suspensions. *Langmuir* **1990**, *6*, 15−24.

(21) Mohebi, M.; Jamasbi, N.; Liu, J. Simulation of the formation of nonequilibrium structures in magnetorheological fluids subject to an external magnetic field. *Phys. Rev. E* **1996**, *54* (5), 5407−5413.

(22) Haghgooie, R.; Doyle, P. S. Transition from two-dimensional to three-dimensional behavior in the self-assembly of magnetorheological fluids confined in thin slits. *Phys. Rev. E* **2007**, *75* (6), 061406.

(23) Kim, Y. J.; Liu, Y. D.; Seo, Y.; Choi, H. J. Pickering-emulsion-polymerized polystyrene/Fe_2O_3 composite particles and their magnetoresponsive characteristics. *Langmuir* **2013**, *29* (16), 4959−4965.

(24) Lopez-Lopez, M. T.; Vertelov, G.; Bossis, G.; Kuzhir, P.; Duran, J. D. G. New magnetorheological fluids based on magnetic fibers. *J. Mater. Chem.* **2007**, *17*, 3839−3844.

(25) Ginder, J. M.; Davis, L. C.; Elie, L. D. Rheology of magnetorheological fluids: Models and measurements. *Int. J. Mod. Phys. B* **1996**, *10* (23 & 24), 3293−3303.

(26) Elfimova, E. A.; Ivanov, A. O.; Camp, P. J. Thermodynamics of ferrofluids in applied magnetic fields. *Phys. Rev. E* **2013**, *88* (4), 042310.

(27) Odenbach, S. Magnetoviscous and viscoelastic effects in ferrofluids. *Int. J. Mod. Phys. B* **2000**, *14* (16), 1615−1631.

(28) Pop, L. M.; Odenbach, S.; Wiedenmann, A.; Matoussevitch, N.; Bonnemann, H. Microstructure and rheology of ferrofluids. *J. Magn. Magn. Mater.* **2005**, *289*, 303−306.

(29) Pinho, M.; Brouard, B.; Genevaux, J. M.; Dauchez, N.; Volkova, O.; Meziere, H.; Collas, P. Investigation into ferrofluid magnetoviscous effects under an oscillating shear flow. *J. Magn. Magn. Mater.* **2011**, *323* (18-19), 2386−2390.

(30) Soto-Aquino, D.; Rosso, D.; Rinaldi, C. Oscillatory shear response of dilute ferrofluids: Predictions from rotational Brownian dynamics simulations and ferrohydrodynamics modeling. *Phys. Rev. E* **2011**, *84*, 056306.

(31) Wyss, H. M.; Miyazaki, K.; Mattsson, J.; Hu, Z.; Reichman, D. R.; Weitz, D. A. Strain-rate frequency superposition: A rheological probe of structural relaxation in soft materials. *Phys. Rev. Lett.* **2007**, *98* (23), 238303.

(32) Mohan, P. H.; Bandyopadhyay, R. Phase behavior and dynamics of a micelle-forming triblock copolymer system. *Phys. Rev. E* **2008**, *77* (4), 041803.

(33) Spruijt, E.; Sprakel, J.; Lemmers, M.; Stuart, M. A. C.; Gucht, J. v. d. Relaxation dynamics at different time scales in electrostatic complexes: Time−salt superposition. *Phys. Rev. Lett.* **2010**, *105* (20), 208301.

(34) Kowalczyk, A.; Hochstein, B.; Stahle, P.; Willenbacher, N. Characterization of complex fluids at very low frequency: Experimental verification of the strain rate-frequency superposition (SRFS) method. *Appl. Rheol.* **2010**, *20* (5), 52340.
(35) Shedge, A. S.; Wadgaonkar, P. P.; Lele, A. K.; Badiger, M. V. Hydrophobically modified poly(vinyl alcohol) using alkoxy-substituted methyl gallate: Synthesis and rheology. *J. Polym. Sci., Part B: Polym. Phys.* **2010**, *48* (10), 1054−1063.
(36) Oliver, M.; Kovats, T.; Mijailovich, S. M.; Butler, J. P.; Fredberg, J. J.; Lenormand, G. Remodeling of integrated contractile tissues and its dependence on strain-rate amplitude. *Phys. Rev. Lett.* **2010**, *105* (15), 158102.
(37) Krishnaswamy, R.; Majumdar, S.; Sood, A. K. Nonlinear viscoelasticity of sorbitan tristearate monolayers at liquid/gas interface. *Langmuir* **2007**, *23* (26), 12951−12958.
(38) Gnanaprakash, G.; Philip, J.; Jayakumar, T.; Raj, B. Effect of digestion time and alkali addition rate on physical properties of magnetite nanoparticles. *J. Phys. Chem. B* **2007**, *111* (28), 7978−7986.
(39) Shima, P. D.; Philip, J.; Raj, B. Synthesis of aqueous and nonaqueous iron oxide nanofluids and study of temperature dependence on thermal conductivity and viscosity. *J. Phys. Chem. C* **2010**, *114* (44), 18825−18833.
(40) Muthukumaran, T.; Gnanaprakash, G.; Philip, J. Synthesis of stable magnetic nanofluids of different particle sizes. *J. Nanofluids* **2012**, *1* (1), 85−92.
(41) Waldron, R. D. Infrared spectra of ferrites. *Phys. Rev.* **1955**, *99*, 1727−1735.
(42) Ahmed, M. A.; Ateia, E.; El-Dek, S. I. Spectroscopic analysis of ferrite doped with different rare earth elements. *Vib. Spectrosc.* **2002**, *30*, 69−75.
(43) Parthasarathy, M.; Klingenberg, D. J. A microstructural investigation of the nonlinear response of electrorheological suspensions II. Oscillatory shear flow. *Rheol. Acta* **1995**, *34*, 430−439.
(44) Parthasarathy, M.; Klingenberg, D. J. A microstructural investigation of the nonlinear response of electrorheological suspensions I. Start-up of steady shear flow. *Rheol. Acta* **1995**, *34*, 417−429.
(45) Ilg, P.; Kröger, M.; Hess, S. Magnetoviscosity of semidilute ferrofluids and the role of dipolar interactions: Comparison of molecular simulations and dynamical mean-field theory. *Phys. Rev. E* **2005**, *71*, 031205.
(46) Weeber, R.; Klinkigt, M.; Kantorovich, S.; Holm, C. Microstructure and magnetic properties of magnetic fluids consisting of shifted dipole particles under the influence of an external magnetic field. *J. Chem. Phys.* **2013**, *139*, 214901.
(47) McTague, J. P. Magnetoviscosity of magnetic colloids. *J. Chem. Phys.* **1969**, *51*, 133.
(48) Haghgooie, R.; Doyle, P. S. Transition from two-dimensional to three-dimensional behavior in the self-assembly of magnetorheological fluids confined in thin slits. *Phys. Rev. E* **2007**, *75*, 061406.
(49) Chirikov, D. N.; Fedotov, S. P.; Iskakova, L. Y.; Zubarev, A. Y. Viscoelastic properties of ferrofluids. *Phys. Rev. E* **2010**, *82*, 051405.
(50) Martin, J. E.; Odinek, J.; Halsey, T. C.; Kamien, R. Structure and dynamics of electrorheological fluids. *Phys. Rev. E* **1998**, *57* (1), 756−775.
(51) McLeish, T. C. B.; Jordan, T.; Shaw, M. T. Viscoelastic response of electrorheological fluids. I. Frequency dependence. *J. Rheol.* **1991**, *35* (3), 427−448.
(52) Ramos, J.; Vicente, J. d.; Hidalgo-Alvarez, R. Small-amplitude oscillatory shear magnetorheology of inverse ferrofluids. *Langmuir* **2010**, *26* (12), 9334−9341.
(53) Mason, T. G.; Weitz, D. A. Linear viscoelasticity of colloidal hard sphere suspensions near the glass transition. *Phys. Rev. Lett.* **1995**, *75* (14), 2770−2773.
(54) Cloitre, M.; Borrega, R.; Leibler, L. Rheological aging and rejuvenation in microgel pastes. *Phys. Rev. Lett.* **2000**, *85* (22), 4819−4822.
(55) Ferry, J. D. *Viscoelastic Properties of Polymers*, 3rd ed.; John Wiley & Sons: New York, 1980.
(56) Cramer, C.; De, S.; Schonhoff, M. Time−humidity−superposition principle in electrical conductivity spectra of ion-conducting polymers. *Phys. Rev. Lett.* **2011**, *107* (2), 028301.
(57) Klingenberg, D. J. Simulation of the dynamic oscillatory response of electrorheological suspensions: Demonstration of a relaxation mechanism. *J. Rheol.* **1993**, *37* (2), 199−214.
(58) Kuzhir, P.; Gómez-Ramírez, A.; López-López, M. T.; Bossis, G.; Zubarev, A. Y. Non-linear viscoelastic response of magnetic fiber suspensions in oscillatory shear. *J. Non-Newtonian Fluid Mech.* **2011**, *166* (7-8), 373−385.
(59) López-López, M. T.; Gómez-Ramírez, A.; Rodríguez-Arco, L.; Durán, J. D. G.; Iskakova, L.; Zubarev, A. Colloids on the frontier of ferrofluids. Rheological properties. *Langmuir* **2012**, *28*, 6232−6245.
(60) Zubarev, A. Y.; Iskakova, L. Y. To the theory of rheological properties of ferrofluids: Influence of drop-like aggregates. *Physica A* **2004**, *343*, 65−80.
(61) Laskar, J. M.; Philip, J.; Raj, B. Experimental evidence for reversible zippering of chains in magnetic nanofluids under external magnetic fields. *Phys. Rev. E* **2009**, *80* (4), 041401.
(62) Felicia, L. J.; Philip, J. Probing of field-induced structures and tunable rheological properties of surfactant capped magnetically polarizable nanofluids. *Langmuir* **2013**, *29* (1), 110−120.
(63) Moctezuma, R. E.; Donado, F.; Arauz-Lara, J. L. Lateral aggregation induced by magnetic perturbations in a magneto-rheological fluid based on non-Brownian particles. *Phys. Rev. E* **2013**, *88* (3), 032305.
(64) Chirikov, D. N.; Fedotov, S. P.; Iskakova, L. Y.; Zubarev, A. Y. Viscoelastic properties of ferrofluids. *Phys. Rev. E* **2010**, *82* (5), 051405.
(65) Kroell, M.; Pridoehl, M.; Zimmermann, G.; Pop, L.; Odenbach, S.; Hartwig, A. Magnetic and rheological characterization of novel ferrofluids. *J. Magn. Magn. Mater.* **2005**, *289*, 21−24.